ARTICLE

ACS chemical biology

Bisphenol A Directly Targets Tubulin to Disrupt Spindle Organization in Embryonic and Somatic Cells

Olivia George[†,§], Bj K. Bryant[‡], Ramesh Chinnasamy[‡], Cesear Corona[‡], Jeffrey B. Arterburn[‡], and Charles B. Shuster[†,§,*]

[†]Department of Biology and, [‡]Department of Biochemistry and Chemistry, New Mexico State University, Las Cruces, New Mexico 88003, and [§]Marine Biological Laboratory, Woods Hole, Massachusetts 02543

ABSTRACT There is increasing concern that animal and human reproduction may be adversely affected by exposure to xenoestrogens that activate estrogen receptors. There is evidence that one such compound, Bisphenol A (BPA), also induces meiotic and mitotic aneuploidy, suggesting that these kinds of molecules may also have effects on cell division. In an effort to understand how Bisphenol A might disrupt cell division, a phenotypic analysis was carried out using sea urchin eggs, whose early embryonic divisions are independent of zygotic transcription. Fertilized *Lytechinus pictus* eggs exposed to BPA formed multipolar spindles resulting in failed cytokinesis in a dose-dependent, transcriptionally independent manner. By use of novel biotinylated BPA affinity probes to fractionate cell-free extracts, tubulin was identified as a candidate binding protein by mass spectrometry, and BPA promoted microtubule polymerization and centrosome-based microtubule nucleation *in vitro* but did not appear to display microtubule-stabilizing activity. Treatment of mammalian cells demonstrated that BPA as well as a series of Bisphenol A derivatives induced ectopic spindle pole formation in the absence of centrosome overduplication. Together, these results suggest a novel mechanism by which Bisphenol A affects the nucleation of microtubules, disrupting the tight spatial control associated with normal chromosome segregation, resulting in aneuploidy.

Xenoestrogens are a structurally diverse class of nonsteroidal compounds that share structural features with steroid hormones and modulate the activity of nuclear hormone receptors (*1*). Although the potencies of xenoestrogens vary, their release into the environment has begun to have a measurable effect on the reproductive development of several species, and there is increasing concern that human reproduction is being affected as well (*2, 3*). One such weakly estrogenic compound that has increasingly become a cause for concern is Bisphenol A (4,4′-isopropylidenediphenol, BPA). Although less estrogenic than diethylstilbestrol (DES), BPA affects male and female reproductive development at low doses, and while much of the research to date has focused on BPA's role as a potential endocrine disruptor (*4, 5*), nongenomic effects have been reported as well (*1, 6*). Nearly ubiquitous, BPA is found extensively in polycarbonate plastics, resins lining food containers, adhesives, and dental sealants, and leaching has been documented with many of these products (*7–9*). One particularly startling finding arose from a rodent colony accidentally exposed to Bisphenol A, where increases in synaptic abnormalities and meiotic aneuploidy were detected in mouse oocytes (*10, 11*). The detection of chromosome congression and meiotic nondisjunction errors in exposed mice suggested that in addition to aberrantly activating the estrogen receptor, Bisphenol A may be directly interfering with the mechanics of cell division.

Like DES, BPA has been reported to transform cells *in vitro* and has been linked to tumor formation in animal models (*12–16*), although genotoxicity assays performed with *Salmonella typhimurium* indicated that BPA

*Corresponding author, cshuster@nmsu.edu.

Received for review July 6, 2007 and accepted December 30, 2007.

Published online January 29, 2008

10.1021/cb700210u CCC: $40.75

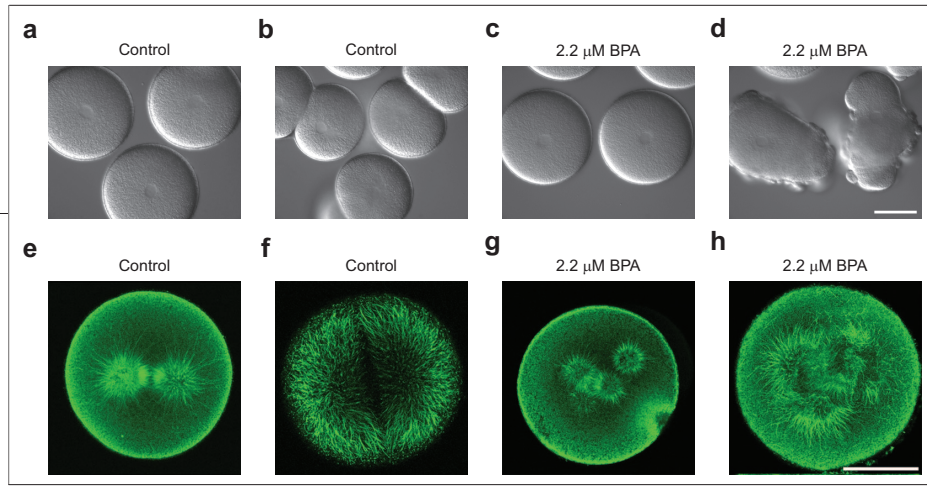

Figure 1. Dose-dependent effects of BPA on microtubule organization and cell division in sea urchin embryos. *L. pictus* eggs were fertilized, stripped of their fertilization envelopes, and cultured through the first division in the presence of 0.1% DMSO (panels a, b, e, and f) or 2.2 μM BPA (panels c, d, g, and h). Note that while the control embryos underwent normal cytokinesis (panel b), BPA-treated embryos formed multiple, misplaced cleavage furrows (panel d). Analysis of microtubule organization in metaphase (panels e and g) and anaphase (panels f and h) embryos revealed the presence of normal metaphase and anaphase spindles in control embryos (panels e and f) but supernumary spindle poles in BPA-treated embryos (panels g and h). Bars in panels d and h represent 50 μm.

is not mutagenic (*17*). Studies in mammary tumor cell lines demonstrated that BPA is able to induce expression of estrogen responsive genes and promote proliferation (*9*), consistent with the notion that BPA promotes cellular proliferation though the estrogen receptor. In contrast, cell lines that lack measurable levels of estrogen receptors are also capable of BPA-induced cellular transformation (*16*). The same study as well as others reported an increase in aneuploidy with BPA exposure (*18–21*) although the concentrations required to induce aneuploidy in cultured cells were much higher than those reported for whole animal studies (*11*). However, alterations in spindle morphology were reported for both cultured somatic cells and oocytes (*18, 21–24*), suggesting that the reported congression failures of chromosomes at metaphase and nondisjunction at anaphase may due to BPA's affect on microtubule assembly and organization. While mechanisms for nondisjunction might be based on BPA and metabolite interactions with DNA (*10, 16, 25–28*), the appearance of altered spindle morphology suggests that BPA may also indirectly or directly target the mitotic apparatus to affect chromosome segregation and the maintenance of ploidy.

Studies concerning the endocrinology and developmental toxicology of BPA suggest that this compound is a potential threat to human health, but none of the studies to date has clearly established a molecular mechanism by which BPA increases aneuploidy through its alteration of the mitotic spindle. In an effort to understand how BPA disrupts the machinery of cell division, we undertook a multidisciplinary approach combining synthetic organic chemistry, imaging, and biochemistry to identify tubulin as a direct target of BPA. In agreement with earlier findings, we find that BPA induces multipolar spindles in diverse cell types and propose a model by which BPA produces multipolar spindles by promoting ectopic microtubule nucleation, disrupting spindle morphology, and ultimately contributing to chromosome segregation defects and aneuploidy.

RESULTS

BPA Alters Microtubule Organization during Early Embryogenesis. BPA has been reported to disrupt mitotic and meiotic divisions, but the molecular mechanisms by which BPA induces aneuploidy remain elusive. Moreover, dramatic discrepancies have been reported between whole animal and cultured cell models for the doses of BPA that induce aneuploidy and spindle disruption (*10, 11, 18, 22*). In an effort to better characterize nongenomic (ER-independent) effects of BPA during mitosis, we undertook a systematic examination of BPA effects on cell division in both embryonic and somatic cells. As a first estimation of the effects of BPA on mitosis, we followed the first embryonic divisions of sea urchin embryos, which have been shown to be sensitive to estrogenic compounds (*29*), but whose early development is transcription-independent (*30*). Fertilized *Lytechinus pictus* eggs were exposed to BPA at concentrations ranging from 200 nM to 5 μM and followed through the first division by differential interference contrast (DIC) time-lapse microscopy (Figure 1, panels a–d). Because exposure to BPA earlier than 20 min postfertilization delayed pronuclear migration and fusion, experimental embryos were cultured in control seawater for 25 min prior to treatment with BPA. In comparison to DMSO controls (Figure 1, panels a and b), BPA-treated embryos formed multiple, ectopic furrows and membrane blebs that later regressed to form spherical, binucleate eggs (Figure 1, panels c and d), suggesting that there were defects in cleavage plane determination. BPA effects on cytokinesis were dose-dependent, with an IC_{50} of 3 μM, but effects were detected as low as 500 nM (Supplemental Figure 1). This dose range was comparable to levels previously described for rodents exposed to BPA (0.44–1.6 μM) (*11*) but lower than what was used on mouse oocytes matured *in vitro* (10–30 μM) (*23*). Early development of the sea urchin

relies on maternal transcripts (*30*), and we found that pretreatment of eggs with 80 μM actinomycin D failed to suppress BPA disruption of cleavage plane determination (not shown), suggesting that hormone-receptor-mediated transcription could not account for the observed cell division defects.

Microtubules of the mitotic apparatus are responsible for specifying the cleavage plane in all animal cells, and in echinoderm embryos, the explosive outgrowth of astral microtubules and their contact with the cortical actin cytoskeleton marks the position of the future contractile ring (*31, 32*). Because embryos exposed to BPA displayed failures in cleavage plane determination and cytokinesis, the organization of the mitotic spindle was examined in control and BPA-treated embryos (Figure 1, panels e–h). Whereas control eggs formed normal bipolar spindles that underwent a stereotypical transition from metaphase to anaphase (Figure 1, panels e and f), eggs exposed to BPA displayed multiple spindle poles, that upon anaphase onset, resulted in a disorganized elongation of astral microtubules toward the cortex (Figure 1, panels g and h). Monopolar spindles were occasionally observed, but unlike the appearance of multipolar spindles, there was no dose-dependent increase in the frequency of monopolar spindles. Because there are several possible mechanisms by which multipolar spindles may form (centrosome amplification, centriole splitting, *de novo* formation, *etc.*), microtubule organization was followed in living cells using orientation-independent polarization microscopy, which allows for visualization of spindle formation without the use of fluorescent probes (*33, 34*). As shown in Figure 2, control embryos underwent normal spindle assembly, as evidenced by the presence of a birefringent bipolar spindle (Figure 2, panels a–c, and Supplemental Movie 1). In BPA-treated cells (Figure 2, panels d–i, Supplemental Movies 2 and 3), supernumery asters could be detected forming *de novo* (Figure 2, panels e, f, h, and i, arrows). As mentioned above, monopolar spindles could also be detected forming near the nucleus following nuclear envelope breakdown (Figure 2, panels e and f, asterisk), but in all 28 cells observed, we failed to observe spindle collapse (which would account for the presence of a monopole).

Design of BPA Probes for Affinity Purification. BPA treatment of sea urchin eggs produced defects in microtubule organization that resulted in cleavage failure

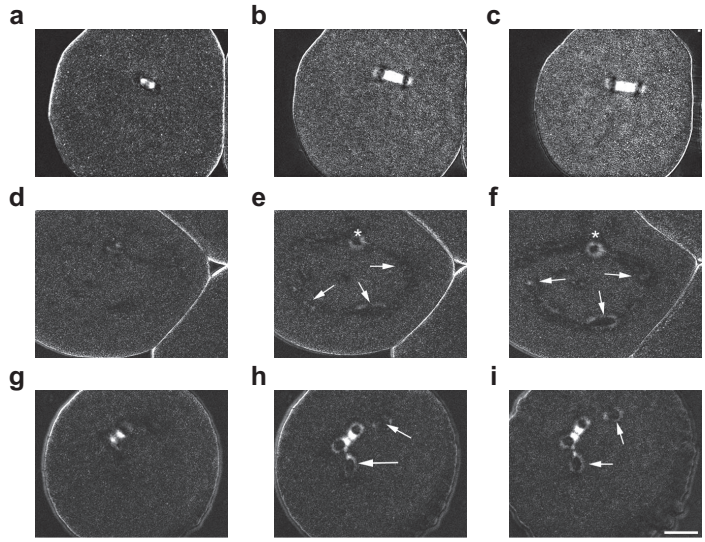

Figure 2. Visualization of ectopic spindle pole formation in BPA-treated sea urchin eggs. *L. pictus* eggs exposed to either DMSO carrier (panels a–c) or 2.2 μM BPA were compressed under fluorocarbon oil to aid in visualizing spindle formation and followed by polarization microscopy. Whereas controls formed normal, birefringent spindles (panels a–c), embryos exposed to BPA could be observed forming monopolar spindles (*) as well as *de novo* microtubule organizing centers in the cytoplasm (panels d–f, arrows). In other cells, asters could be observed splitting off the main spindle (panels g–i, arrows). Bar represents 20 μM.

(Figures 1 and 2) but had no other effects on cell cycle timing or progression. In order to identify cellular targets of BPA that may be involved in the observed dose-dependent effects on dividing cells, we initiated efforts to design a BPA affinity probe. The presence of a polar, acidic phenol group connected to a hydrophobic aliphatic backbone is a key feature of BPA that is recognized in structure–activity models of estrogenicity (*35–37*), and we anticipated that these characteristics would also be essential for binding other proteins. The standard procedure for biotinylation involves coupling a nucleophilic residue on the substrate, typically an amine or thiol group, with an activated carboxylate or maleimide derivative of biotin, respectively. BPA lacks suitable reactive functional groups of this type and possesses a nonpolar backbone that likely interacts with hydrophobic protein binding sites. The design of small molecule affinity probes requires judicious introduction of functionality for conjugation to avoid adversely affecting the binding affinity due to unfavorable electrostatic interactions, modified solvation characteristics, altered lipophi-

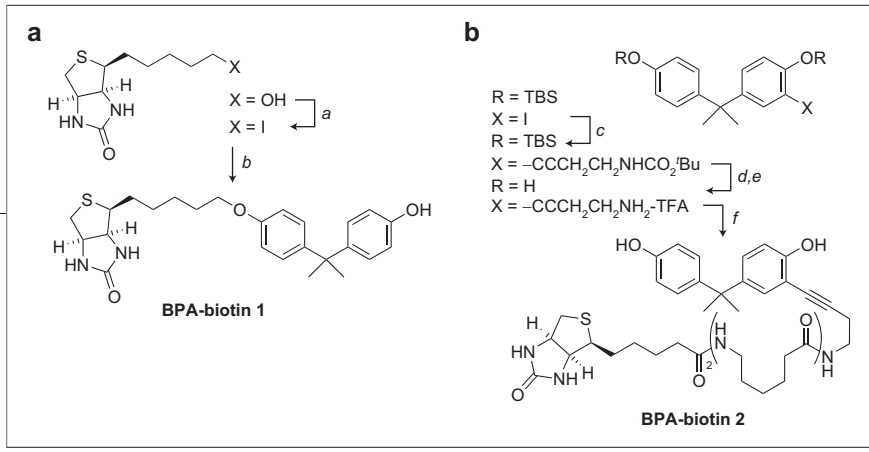

Figure 3. Synthesis of BPA–biotin affinity probes. a) The BPA–biotin derivative 1 was prepared by Williamson ether synthesis. The 5-hydroxy derivative was converted to 4-(5-iodopentyl) tetrahydro-1*H*-thieno[3,4-*d*]imidazol-2(3*H*)-one using I_2, triphenylphosphine. Selective O-alkylation of BPA with the primary alkyl iodide gave the desired compound 1 as the major product. b) The BPA–biotin derivative 2 was prepared by sequential Sonogashira coupling and biotinylation. 4-(2-(4-Hydroxyphenyl)propan-2-yl)-2-iodophenol was protected as the bis-TBS ether using standard conditions and was then coupled with *tert*-butylbut-3-ynylcarbamate to the alkyne product in excellent yield. The TBS protecting groups were removed with TBAF, and the ^{t}Boc group was cleaved with TFA to provide the corresponding ammonium salt. Biotinylation with biotin-L_2-NHS in Et_3N/DMF gave the desired compound 2. Both of the biotinylated probes 1 and 2 were purified by silica gel chromatography and structurally characterized by ^{1}H and ^{13}C NMR and HPLC-MS. Details of probe syntheses are available as Supporting Information.

licity, and increased steric interactions. We have recently described an alternative approach for the biotinylation of hydrophobic substrates that replaces the carboxylic group with a nonpolar linkage to the 7-oxo-3-thia-6,8-diazabicyclo[3.3.0]oct-4-yl heterocycle that provides the major contribution to (strept)avidin binding affinity (*38*). Extending this approach, we designed two types of BPA probes (Figure 3). Compound **1** (BPA–biotin 1) possesses a phenolic ether connection to a reduced biotin fragment and provides minimal alteration of BPA's hydrophobic backbone (Figure 3, left panel). Compound **2** (BPA–biotin 2) incorporates a butynyl carboxamide as a spacer group attached at the ortho position of the aryl ring that preserves both of the phenol groups found in the original BPA (Figure 3, right panel).

Identification of Tubulin as a BPA-Binding Protein. Biotin-linked analogues of BPA were used to fractionate cell-free extracts derived from *Xenopus* oocytes. The highly concentrated extracts of frog and clam oocytes are capable of replicating microtubule and centrosomal dynamics that mirror the *in vivo* state and have been used extensively for the study of cytoskeletal and cell cycle dynamics (*39–41*). *Xenopus* cytostatic factor (CSF)-arrested extracts were incubated in the presence of BPA–biotin **1** or **2**, bound complexes were collected using streptavidin–agarose, and those proteins specifically interacting with BPA were eluted with 210 μM free BPA and resolved by SDS-PAGE (Figure 4, panel a). Two bands of interest were identified that eluted with BPA from BPA–biotin matrices (Figure 4, panel a, fractions F2 and F3, denoted by ∗ and +) but not from biotin alone (not shown). MALDI-TOF analysis identified the upper band as aconitase and the lower band (denoted with +) as α,β-tubulin. While the purification of aconitase was batch-dependent, α- as well as γ-tubulin consistently eluted from both of the BPA–biotin affinity probes as detected by Western blotting (Figure 4, panel b, fractions F2–F8), and was independent of the extract fractionated (*Xenopus*, sea urchin, or surf clam). In contrast, neither α- nor γ-tubulin eluted from biotin control matrices (Figure 4, panel b, fractions F2–F8). Centrosomal components, such as pericentrin and ϵ-tubulin, were not detected eluting from BPA affinity matrices, suggesting that centrosomes or centrosomal precursors were not associating with the matrix as a complex (not shown). To validate tubulin as a target for BPA, tubulin was polymerized in the presence of increasing concentrations of BPA and followed by fluorimetry (Figure 4, panel c). Because DMSO alone can promote microtubule polymerization, methanol was used as a solvent, which had no effect on microtubule polymerization (at 0.14%). As shown in Figure 4c, BPA promoted microtubule polymerization, although to a lesser extent than the potent microtubule stabilizer, taxol (Figure 4c, solid lines). BPA-induced microtubule polymerization could be detected in the presence of 20% glycerol, where glycerol acts as a general stabilizer of microtubules (*42, 43*). In contrast, microtubule polymerization in the presence of 10-fold less glycerol was undetectable in either control or BPA-treated samples (Figure 4, panel c, dashed lines), whereas taxol-treated samples polymerized normally. The requirement of glycerol for BPA-induced microtubule polymerization suggested that BPA may not be stabilizing microtubules in the same manner as taxol, and this was further confirmed when BPA failed to protect microtubules from depolymerization by cold treatment or 4 mM $CaCl_2$ (not shown). Thus, while BPA was capable of promoting microtubule polymerization *in vitro*, it did not appear to act as a stabilizer.

In vitro, BPA promoted microtubule polymerization but did not appear to act as a microtubule stabilizer in comparison with taxol. To better understand the action of BPA on microtubule polymerization, we followed centrosome-nucleated aster formation in the absence or presence of BPA. CSF extracts were supplemented

with rhodamine-tubulin, sperm nuclei, and BPA or carrier control, warmed to 15 °C for 10 min, and fixed onto slides. While a small amount of nucleation at the centrosome was detected in controls under these conditions (Figure 5, panel a), BPA-treated extracts (Figure 5, top, panels b–d) displayed a 5.7-fold increase in aster size at concentrations as low as 500 nM (Figure 5, panels a and b). Small but statistically significant increases could be detected at higher doses (Figure 5, panel b), and at concentrations above 10 μM, noncentrosomal microtubule nucleation appeared to predominate in the extracts and sperm asters became more disorganized and difficult to quantify (not shown). The robust nucleation of microtubule asters observed in the presence of 500 nM BPA contrasted sharply with the modest promotion of microtubule polymerization observed with purified tubulin at the same BPA concentration (Figure 4, panel c) suggesting that BPA promoted microtubule nucleation.

BPA Induction of Acentriolar Spindle Poles. In animal cells, interphase and mitotic microtubule arrays are organized by centrosomes, which serve as a scaffold for γ-tubulin-based microtubule nucleation and anchoring (*44*). BPA bound both α/β- and γ-tubulin *in vitro* (Figure 4) and altered microtubule organization in dividing sea urchin eggs (Figures 1 and 2), but the mechanisms by which these alterations occur were still not clear. We revisited BPA's effects on microtubule organization in mammalian cells (Figure 6), where BPA has been shown to act as a disruptor of microtubule organization in cultured mammalian cells and oocytes (*18, 22, 23*), albeit at much higher concentrations than what we and others have observed for oocytes and early embryos (*11, 23*). In HeLa cells, microtubule stabilizers such as taxol suppress microtubule dynamics, resulting in microtubules of uniform length during both interphase and mitosis (Figure 6, panels b and f). In contrast, BPA had no affect on interphase microtubule organization (Figure 6, panels c and d) at any concentration ranging from 500 nM to 200 μM, and BPA did not induce the small ectopic asters associated with taxol (Figure 6, panel f). Instead, BPA induced the dose-dependent formation of ectopic spindle poles (Figure 6, panels g and h; and Figure 7, panel b) with an IC_{50} of 100 μM in a manner that was independent of the carrier used to solubilize BPA (DMSO or MeOH). The vast majority of cells observed (>90%, $n = 400$) contained only one or two additional poles, and consistent with earlier reports (*18, 21*), these cells were able to progress through anaphase and initiate cytokinesis, cleaving into three or four daughter cells (not shown). Additionally, both biotin conjugates were capable of inducing ectopic poles (Figure 6, panels m and n), as were Bisphenol A monomethyl ether (**BPA-Me**) and Bisphenol A dimethyl ether (**BPA-Me$_2$**) (Figure 6, panels o and p). These BPA ethers have 1.6- and 184-fold lower affinity for the estrogen receptor, respectively (*45*), yet there was no significant reduction in the ability of these analogues to induce mul-

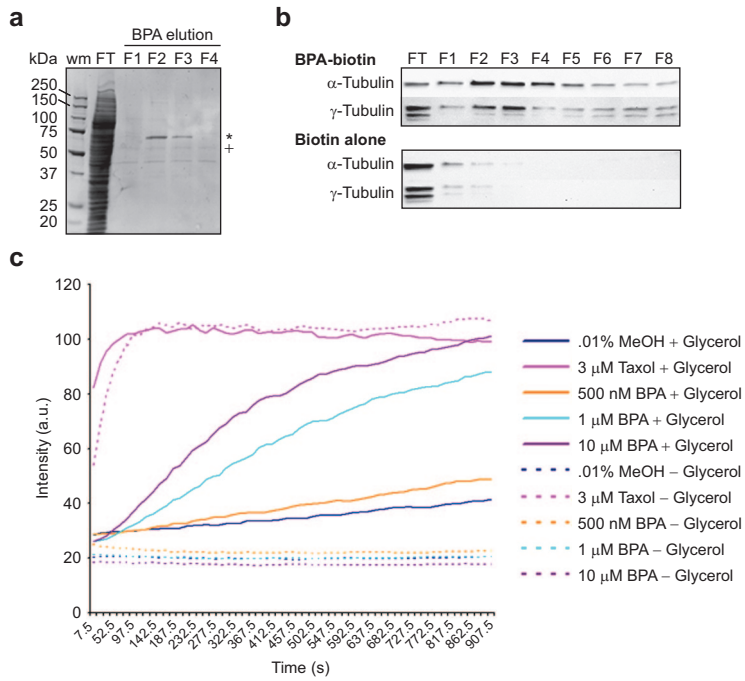

Figure 4. BPA binds tubulin and promotes microtubule polymerization. a) CSF-arrested *Xenopus* extracts (XE) were incubated with biotinylated BPA (BPA-biotin 1), and protein complexes were fractionated over strepavidin beads. Following the collection of the flow-through (FT) fraction and washing with BRB80 buffer, bound proteins were eluted (fractions F1–F4) with 210 μM BPA. Bound proteins were then resolved on a 4–15% SDS-PAGE gradient gel. Two bands were chosen for analysis and sequencing (* and +), and the band denoted by (+) was identified by mass spectroscopy as α-/β-tubulin. b) Western blot confirmation of α-tubulin and γ-tubulin elution from BPA–biotin 1 affinity matrices in fractions 1–8 (FT corresponds to the flow-through or unbound fraction). In contrast, extract incubated with biotin alone showed that neither α-tubulin or γ-tubulin associated with the affinity matrix. c) Tubulin was polymerized in the presence of 20% glycerol (solid lines) in the presence of either carrier alone (0.1% MeOH), 3 μM taxol, or increased concentrations of BPA. A parallel set of assays were performed in the presence of low glycerol (2%), where microtubules polymerize poorly unless in the presence of an additional stabilizing reagent (dashed lines). Samples were assembled on ice and warmed to 37 °C, and readings were acquired every 15 s. Note that while taxol-induced polymerization was independent of glycerol, BPA-induced polymerization did not occur in the absence of glycerol.

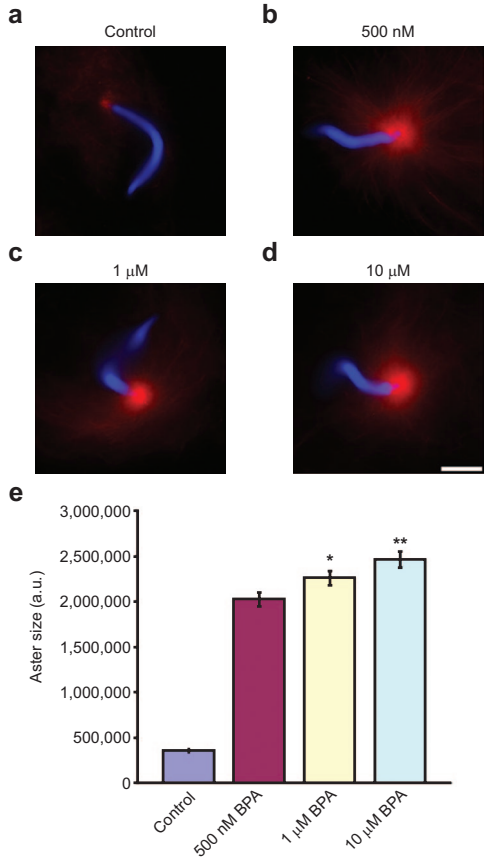

Figure 5. BPA promotes microtubule nucleation from centrosomes *in vitro*. a–d) CSF-arrested *Xenopus* CSF extracts were incubated with sperm nuclei, rhodamine tubulin, and carrier control (0.8% MeOH) or BPA for 30 min on ice. Tubes were then warmed to 15 °C for 10 min. Reactions were stopped by adding 1 μL of each reaction to 3 μL of fixative containing Hoescht 33342 and observed by widefield epifluorescence. When compared with controls (panel A), BPA-treated extracts displayed robust microtubule nucleation from centrosomes (panels b–d). Bar represents 10 μm. e) Quantification of BPA-enhanced aster formation in CSF *Xenopus* extracts. The area for single asters was calculated by first normalizing the background and then creating a threshold image. The areas were then calculated using ImageJ for 12 asters per condition. Small but significant differences could be detected between 500 nM and 1 μM BPA ($p = 0.03$, asterisk) as well as between 1 and 10 μM ($p = 0.01$, double asterisk). Error bars denote standard error.

tipolar spindles (Supplementary Figure 2). Consistent with BPA, perturbations were only observed in mitotic cells (Figure 6, panels m–p), with interphase microtubules remaining morphologically normal (Figure 6, panels i–l). Together, these results indicated that both the biotin conjugates as well as analogues with lowered affinity for the estrogen receptor retained biological activity, suggesting that BPA's effects on spindle morphology were extragenic.

Multipolar spindles are commonly found in tumor cell lines, and these defects typically arise due to uncoupling of the centrosome duplication cycle from normal cell cycle controls (*46, 47*). Our data (Figures 1, 2, and 6) as well as other reports have demonstrated the presence of multipolar spindles in cells exposed to BPA (*18, 22*), and the centrosomal component γ-tubulin was found to associate with BPA affinity matrices (Figure 4, panel b), raising the possibility that BPA was inducing centrosome amplification. Given that spindle poles can self-organize in cell-free extracts or whole cells in the absence of centrosomes (*48, 49*), we sought to discriminate between those two possibilities by counting separated centrosomes at the G_2/M transition, as well as the percentage of metaphase multipolar spindles in the absence or presence of BPA (Figure 7). Analysis of separated centrosomes revealed that even in the presence of 200 μM BPA, where nearly 70% of metaphase spindles are multipolar (Figure 7, panel b), cells contained the normal complement of maturing centrosomes in late G2/early prophase (Figure 7, panels a and b). Further, centrin and γ-tubulin localization revealed that for metaphase cells containing supernumerary spindle poles, only two poles contained centrin foci (Figure 7, panel c, micrographs i′–l′), and optical sectioning at 0.5 μm intervals through the cell failed to locate additional foci (not shown). Those spindle poles lacking centrin did contain γ-tubulin, but staining was diffuse (Figure 7, panel c, micrograph k′) in comparison with centrin-positive controls (Figure 7, panel c, micrograph g′). Those multipolar spindles that did contain more than two centrin foci (21%) were not significantly different than controls, suggesting that spindle pole splitting or centrosome amplification was not responsible for the aberrant pole formation in BPA-treated cells.

DISCUSSION

There is an emerging body of evidence that estrogenic phenols such as DES and BPA are carcinogenic, even though BPA fails to demonstrate mutagenicity by Ames testing (*17, 50*). BPA has been demonstrated to cause aneuploidy both in cell culture and in animal models

(*11, 15, 16, 18, 24*), and while it is debatable whether aneuploidy is a causative or aggravating factor in tumorigenesis (*51, 52*), the sensitivity of maturing mammalian oocytes to low concentrations of these compounds (*10, 11*) necessitates a mechanistic reexamination of BPA's effects on mitosis. Using a chemical biological approach, we report here that BPA disrupts mitosis and cytokinesis by inducing the formation of ectopic microtubule organizing centers. Using biotinylated analogues of BPA, we have identified tubulin as a direct target of BPA, which was validated by demonstrating that BPA promoted microtubule polymerization and nucleation *in vitro* (Figures 4 and 5). And while our data does not definitively demonstrate the mechanism by which ectopic spindle poles are generated *in vivo*, these findings lend further credence to the notion that BPA is capable of disrupting normal cellular processes by mechanisms independent of the estrogen receptor.

Identification of BPA Binding Proteins Using Biotinylated Analogues. BPA is a structurally simple compound, which complicates the identification of critical functional groups as well as cellular targets. Because there are dozens of possible targets that participate in spindle assembly and cleavage plane determination (*53–56*), we chose a chemical biological approach to distinguish novel cellular targets using synthetic BPA—biotin conjugates as affinity agents. The biotinylation of proteins and nucleic acids is a mature technology, yet relatively few applications employing biotinylated analogues of small bioactive molecules to identify protein targets have been described. Several biotinylated steroid hormones conjugates have been generated, primarily as immunoassay probes (*57–70*), with relatively few examples using these reagents to study binding with cellular receptors (*71–73*). The potential value of this approach is evident in recent reports employing biotinylated analogues of small molecules to identify penicillin-binding proteins and targets of anti-inflammatory drugs, and investigate the actions of cancer drugs targeting DNA methyltransferases (*74–76*). We

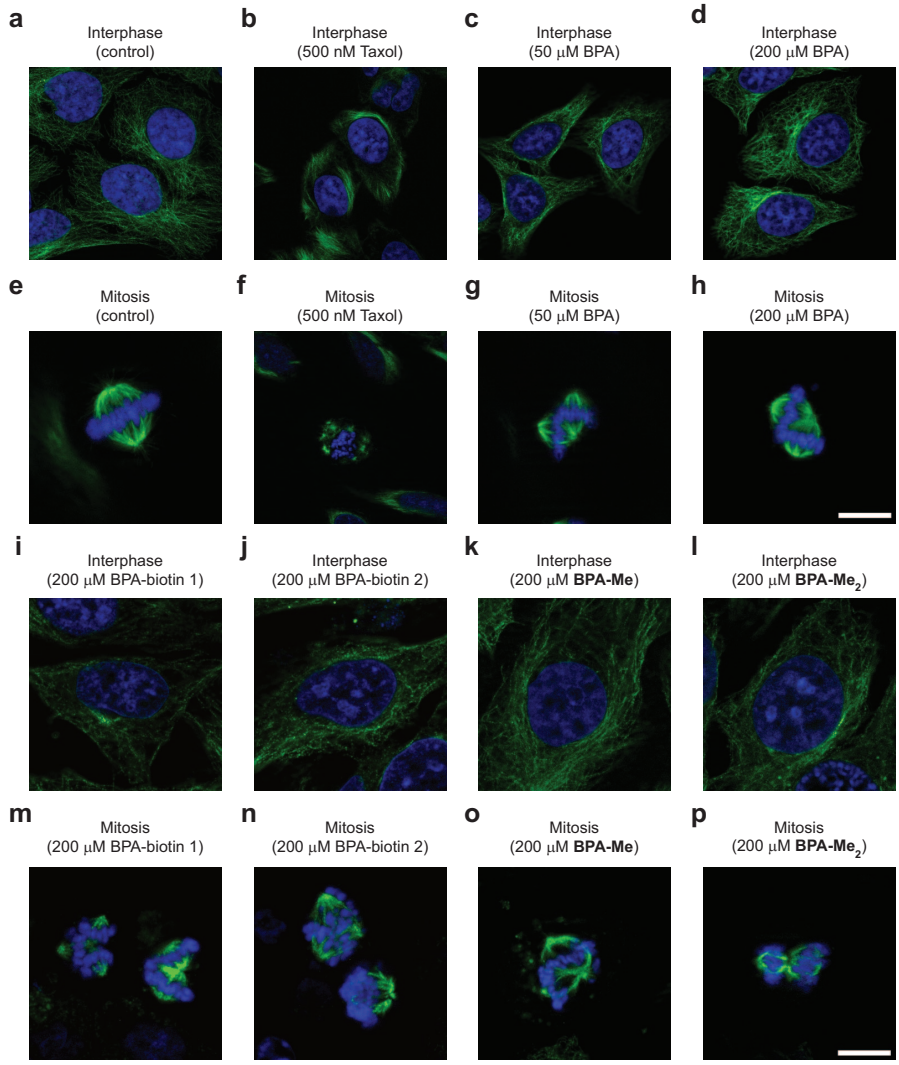

Figure 6. Ectopic spindle pole formation in HeLa cells exposed to BPA. Hela cells were exposed to 0.1% DMSO (panels a and e), 500 nM taxol (panels b and f) or BPA (panels c, d, and f—h), BPA-biotin 1 (panels i and m), BPA—biotin 2 (panels j and n), BPA-Me **(panels k and o), and** BPA-Me_2 **(panels l and p) for 4 h and processed for DNA (blue) and tubulin (green) localization, and representative images were acquired from cells in interphase (panels a—d and i—l) and mitosis (panels e—h and m—p). In contrast to taxol-treated cells (panels b and f) that displayed small, stellate asters, BPA-treated cells developed ectopic spindle poles (panels g and h). Similarly, biotinylated-BPA analogues produced phenotypes consistent with the parent molecule (panels m and n), as did methylated BPA analogues** BPA-Me **and** BPA-Me_2 **(panels o and p). Bar represents 10 μm.**

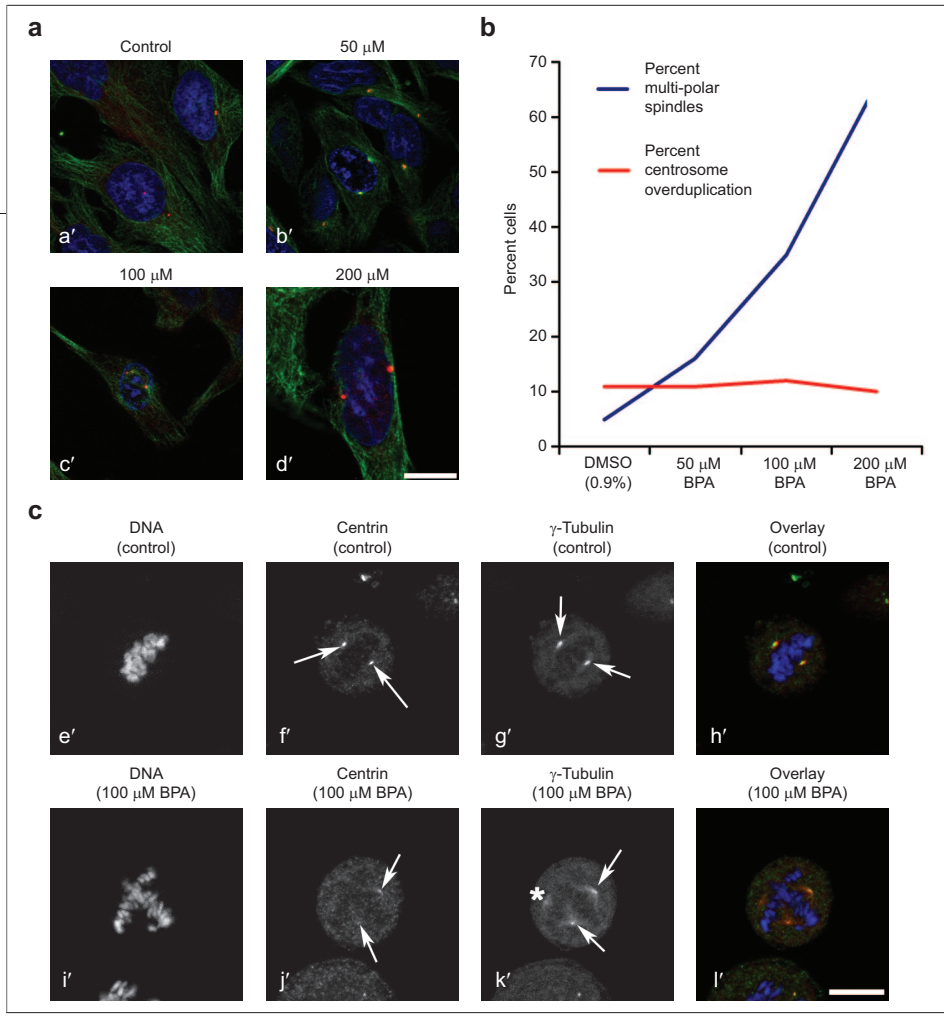

Figure 7. BPA does not drive centrosome amplification to generate ectopic spindle poles. Hela cells were exposed to either 0.1% DMSO or increasing doses of BPA for 4 h, fixed, and processed for DNA (blue), tubulin (green), and pericentrin (red) localization (panel a, micrographs a′–d′; bar, 10 μM). Cells were then scored for the presence of multipolar spindles or centrosomes at the G_2/M transition (panel b). Note that the number of pericentrin-positive centrosomes at G_2/M does not increase even at 200 μM, where the majority of metaphase spindles are multipolar. c) Centrin and γ-tubulin localization in control- (micrographs e′ through h′) and BPA-treated eggs (micrographs i′–l′). Compared to controls (micrographs f′ and g′, arrows), BPA-treated cells contained spindle poles that were positive for both γ-tubulin and centrin (micrographs j′ and k′, arrows), as well as diffuse poles that lacked centrin foci (asterisk k′). Bar represents 10 μm.

recently reported a new strategy for connecting biotin fragments to nonpolar substrates (*38*) and have adapted this approach for BPA to design two types of probes (Figure 3). Compound **1** (BPA-biotin 1) uses one of the phenolic oxygens for construction of a nonpolar ether linkage directly attached to a short biotin fragment, whereas **2** (BPA–biotin 2) incorporates a butynyl spacer attached to the ortho position of the phenol and connected to biotin using an extended linkage. **1** retains one polar phenol and avoids modification of the nonpolar backbone of BPA, while **2** exhibits both of the phenolic groups of BPA and uses the aryl backbone to attach an extended biotin appendage. We anticipated that both probes incorporated key structural elements of BPA and would be viable candidates for affinity purification of protein targets.

Using this approach, we were able to identify α/β- and γ-tubulin by affinity fractionation of *Xenopus* oocyte extracts (Figure 4), and both probes effectively bound tubulin with little observable difference using this qualitative assay (not shown). Additionally, these probes and simple methyl ether derivatives were efficacious in disrupting bipolar spindle organization in cultured cells (Figure 6). These results suggest that hydrophobic interactions of the BPA analogues are responsible for tubulin binding affinity. These observations may also indicate the likelihood that this contact occurs at surface accessible sites of the protein, since both BPA–biotin probes, incorporating short or extended linkages, exhibited affinity for α/β- and γ-tubulin. To date, this is the first report using a solid phase reagent for identifying BPA-binding proteins, and it is possible that this type of analogue may be used for identifying additional targets. These findings also raise the possibility that probes can be designed to distinguish BPA-induced ER-activation from extragenic effects on tubulin nucleation.

BPA Modulation of Microtubule Dynamics and Organization. Affinity fractionation of *Xenopus* extracts identified tubulin as a BPA-associated protein, and *in vitro* analyses demonstrated that BPA directly affected microtubule assembly (Figures 4 and 5). Earlier studies had suggested that both DES and BPA disrupted microtubule organization by promoting microtubule disassembly (*19, 20, 24, 77–80*), which stands in contrast to both our *in vitro* and *in vivo* studies.). While BPA promoted microtubule assembly *in vitro*, it required glycerol and, in contrast to taxol, could not stabilize microtubules in its absence (Figure 4, panel c). BPA also failed to stabilize microtubules against cold or calcium treatment, arguing further against its action as a microtubule stabilizer. BPA's effects *in vivo* in echinoderm embryos and cultured cells was also not consistent with microtu-

bule stabilizers such as taxol or hexylene glycol, with the most notable difference being that BPA had no effect on interphase microtubule organization even at concentrations as high as 0.2 mM (Figures 6 and 7). In contrast, at concentrations that had only a modest effect on the polymerization of purified tubulin, BPA robustly promoted microtubule nucleation from sperm centrosomes (Figure 5), suggesting that BPA was a facilitator of microtubule nucleation.

BPA's effects on the microtubule cytoskeleton appear to be limited to mitosis. During the G_2/M transition, microtubule dynamics undergo a dramatic increase in nucleation and turnover (*81*). *In vitro*, BPA promotes microtubule nucleation (Figure 5), raising the possibility that in mitotic cells, BPA may uncouple nucleation from the centrosome, where nucleation rates are already accelerated.

BPA has been reported to induce multipolar spindles (*18, 22, 23*), and exposure of maturing bovine oocytes with estradiol produces a very similar affect (*82*). Indeed, the estrogen receptor can directly induce the expression of Aurora A kinase (*83–88*), whose overexpression can drive centrosome amplification in many tumor types (*86, 87, 89, 90*). However, we found no evidence for centrosome amplification in cells at the G_2/M boundary, nor did we find centrin localized to ectopic spindle poles (Figure 7). Lastly, methylated BPA analogues with diminished affinity for the estrogen receptor retained the capacity to induce spindle malformations (Figure 6 and Supplementary Figure 2), arguing against the involvement of the estrogen receptor as an indirect mediator of centrosome amplification in BPA-treated cells.

How does BPA induce ectopic spindle poles? Live cell analysis in sea urchin eggs suggests that ectopic asters may form *de novo* (Figure 2, panels e, f, h, and i). Alternatively, ectopic spindle poles may occur *via* spindle pole splitting, where the paired centrioles at one pole split and separate to form a new spindle pole. In sea urchin eggs, this is commonly observed during prolonged mitotic arrest (*91, 92*) or in response to β-mercaptoethanol (*93*). However, because BPA-induced ectopic poles in HeLa cells lacked centrin (and therefore centrioles) (Figure 7, panel c), and the levels of centrin-positive supernumerary poles were no different than carrier controls (not shown), we find little evidence for spindle pole splitting. Furthermore, mammalian oocytes are acentriolar, so it is unlikely that the spindle defects observed in mammalian oocytes are due to centriole splitting *per se* (*11, 23*). However, given that γ-tubulin was also identified eluting from the BPA–biotin affinity matrices (Figure 4), its possible that centrosome fragmentation due to BPA's effects on γ-tubulin could account for the generation of supernumerary spindle poles in centriolar spindle poles in both sea urchins and cultured cells, as well as in acentriolar spindles in mammalian cells. Moreover, centrosomes are not an absolute requirement for pole formation, and studies in *Xenopus* extracts, *Drosophila* embryos, and cultured mammalian cells have demonstrated that centrosomes are dispensable for spindle formation (*48, 94, 95*). Indeed, both whole cells and *Xenopus* extracts are capable of organizing microtubule minus ends in the absence of centrosomes through a mechanism involving dynein and NUMA (*49, 96–98*). In such a self-organization model, kinetochore fibers nucleated and organized by active RanGTPase and further stabilized by BPA would become focused into ectopic spindle poles through a process of NUMA/dynein-mediated organization of microtubule minus ends. Ongoing efforts will determine whether this, indeed, is the case.

METHODS

Embryo and Mammalian Cell Culture. *Lytechinus pictus* sea urchins were obtained from Marinus Scientific (Garden Grove CA) and maintained in a chilled saltwater aquarium at 15 °C. Eggs or sperm were obtained by injecting urchins with 0.5 M KCl and collected gametes used immediately for all experiments. Eggs were fertilized with freshly diluted sperm, and fertilization envelopes were removed by passage through 105 μm Nytex several times before culturing in calcium-free seawater (CaFSW) at 15 °C.

HeLa cells were cultured in Dulbecco's modified Eagle's medium supplemented with 10% fetal calf serum, sodium pyruvate, sodium bicarbonate, and penicillin–streptomycin–fungizone. For BPA treatments, cells were treated with either carrier (0.1% DMSO) or BPA prediluted in media for 3 h prior to fixation by immersion in methanol at −20 °C.

General Chemical Methods. Unless noted otherwise, all chemicals were purchased from Sigma (St. Louis, MO). BPA was dissolved fresh in DMSO or methanol at a concentration of 44 mM and used immediately. Succinimidyl-6-(biotinamido)-6-hexanamido hexanoate (Biotin-L_2-NHS) was purchased from Pierce. The Bisphenol A dimethyl ether (**BPA-Me$_2$**) (1,1′-(1-methylethylidene)bis[4-methoxybenzene]) and Bisphenol A monomethyl ether (**BPA-Me**) (4-[1-(4-methoxyphenyl)-1-methylethyl]phenol) were prepared by methylation of BPA using sodium hydride and methyl iodide in dimethylformamide. Detailed methods of the synthesis of the BPA affinity probes **1** and **2** are included in the Supporting Information.

Live Cell Microscopy. *Lytechinus pictus* eggs were fertilized, stripped of their fertilization membranes, and incubated in CaFSW at 15 °C for 25 min. After 25 min, embryos were treated with varying concentrations of DMSO or BPA and incubated for another 30 min. Cells were then followed by Nomarski/DIC or polarization microscopy. To better visualize the spindle in living cells, control or BPA-treated eggs were settled onto protamine sulfate coated glass-bottomed 35 mm dishes (World Precision Instruments, Sarasota, FL), and compressed under Fluorinert FC-40 oil (*99, 100*). Time-lapse sequences were acquired using Zeiss Axiovert 200 M inverted microscopes configured for either standard Nomarski/DIC or orientation-independent polarization microscopy with a circular polarizer and 546 nm filter placed above the condenser and a liquid crystal universal compensator (LC-Polscope, Cambridge Research Instruments, Woborn MA) placed below the reflector turret. An EXFO X-Cite 120 light source (Mississuaga, ON) was used for transillumination, and images were acquired using a Q Imaging CCD camera controlled by PSJ software (Marine Biological Laboratory, Woods Hole, MA). Image stacks were acquired using a 3 nm retardance ceiling, exported as 8-bit tif files to ImageJ, where movies and figures were then prepared.

Immunofluorescence. Eggs and early embryos were fixed and processed for tubulin localization according to previously described methods (*100, 101*). Hela cells were fixed by immersion in cold methanol for 30 min at −20 °C before rehydration in phosphate-buffered saline (PBS). Both sea urchin eggs and HeLa cells were blocked by incubation in PBS containing 5% bovine serum albumin (blocking buffer), for 1 h at RT. Cells were then placed into 1:1000 dilutions of mouse antitubulin (Sigma) in blocking buffer overnight at 4 °C. In experiments with cultured cells, cells were also counterstained with 1:100 rabbit anticentrin (Sigma) or 1:500 rabbit antipericentrin (Covance, Berkeley, CA). Primary antibodies were detected using Alexafluor-conjugated secondary antibodies (Molecular Probes, Eugene OR). After being washed, cells were mounted in 90% glycerol/1× PBS and stored at −20 °C. Sea urchin embryos were imaged using an Olympus Fluoview confocal microscope at the Central Microscopy Facility at the Marine Biological Laboratory, and HeLa cell images were acquired using a Zeiss Axiovert 200 M inverted microscope equipped with epifluorescence optics and an ApoTome structured illumination module (Carl Zeiss, Thornwood, NY). All acquired images were exported into 8-bit tif files, and figures were prepared using ImageJ and Adobe Photoshop software.

Cell-Free Extract Preparation. Cytostatic factor arrested *Xenopus* oocyte cell-free extracts were prepared according to previously published protocols (*102*). Extracts were clarified by spinning at 16,000 rpm in 4 °C for 10 min. After debris and lipids were separated, proteinase inhibitors (20 μg/mL), cytochalasin D (0.4 μg/mL), and 20X energy mix (3 M creatine phosphate, 0.4 M ATP, pH 7.4, 40 mM EGTA, pH 7.7, and 0.4 M $MgCl_2$) were added to the extract, which was used immediately or supplemented with 150 mM sucrose and snap frozen in liquid nature for later use.

Cell-free extracts were prepared from fertilized sea urchin eggs 30 min postinsemination according to ref 103 and stored at −80 °C until use. Extracts were also prepared from activated *Spisula solidissma* surf clam oocytes according to previously published protocols (*104, 105*), snap frozen, and stored at −80 °C until use.

Affinity Fractionation of BPA-Binding Proteins. *Xenopus* cytoplasmic extracts were thawed and then clarified by centrifugation at 16,000 rpm in 4 °C for 10 min. Fifty microliters of 1 mg mL^{-1} BPA−biotin 1 or 2 or biotin alone was added to 500 μL of clarified extract and incubated at 4 °C for 20 min. A 150 μL portion of Strepavidin beads in a 30% slurry in wash buffer (BRB80 + proteinase inhibitors + 0.2 M ATP) was added to the extracts and incubated at 4 °C for an additional 20 min. The suspension was allowed to settle in a column, and the flow-through fraction was collected and washed with 10 mL of cold wash buffer. To specifically elute BPA-binding proteins, the column was eluted with 210 μM BPA in wash buffer, and 300 μL fractions were collected, snap frozen with liquid nitrogen, and stored at −80 °C. Fractions were resolved on 4–15% SDS-PAGE gradient gels (Bio-Rad, Hercules, CA), and bands were visualized using SYPRO-RUBY (Invitrogen, Carlsbad, CA). For proteomic analysis, unstained gels were washed twice for 10 min in deionized water, incubated in Biosafe Coomassie Stain (Bio-rad) for 1 h, and then destained with deionized water overnight. Under a clean hood, bands of interest were carefully excised and placed into a methanol-washed microcentrifuge tube. Proteolysis, peptide recovery and MALDI-TOF analysis were performed at the Baylor College of Medicine Protein Chemistry Facility.

Measuring Effects of Bisphenol A on Microtubule Polymerization *in Vitro*. Microtubule polymerization in the presence of taxol or BPA was monitored using a fluorescence-based, commercially available assay from Cytoskeleton (Denver, CO). Because DMSO alone is capable of promoting microtubule polymerization at concentrations above 0.2%, BPA was reconstituted in methanol and further diluted in deionized water for the assay. In some conditions, glycerol in the polymerization buffer (20% glycerol, 80 mM PIPES, 0.5 mM EGTA, 2 mM $MgCl_2$, pH 6.9) was reduced to 2% to determine whether BPA acted as a microtubule stabilizer. Reactions were kept on ice until added to a 50 μL cuvette and warmed to 37 °C. Microtubule polymerization was monitored in a temperature-controlled Carey Eclipse fluorescence spectrophotometer (Varian, Inc., Walnut Creek, CA) for 15 min, with readings acquired every 15 s. Data were imported into a Microsoft Excel spreadsheet for further analysis and graph generation.

Microtubule nucleation was followed in *Xenopus* CSF extracts by supplementing thawed extracts with 20X energy mix, 60 μg/mL Rhodamine-tubulin (Cytoskeleton), and demembranated sperm nuclei and stored on ice. BPA was solubilized in methanol and further diluted to 50× stocks in BRB80 buffer. Extracts were supplemented with BPA, preincubated on ice for 30 min, and warmed to 15 °C for 10 min. One microliter of each reaction was mixed with 3 μL of fixative containing Hoescht 33342 and mounted for imaging. Images were acquired using a Zeiss Axiovert 200 M inverted microscope equipped with a 63× NA 1.4 planapo objective and exported into 8-bit tif files, and figures were prepared using ImageJ and Adobe Photoshop software. For quantification of BPA-induced asters, 8-bit images of single asters were normalized for background, aster size was quantified using ImageJ software, and statistical analyses were performed using a pairwise Student's *t* test.

Acknowledgment: The authors thank Snezna Rogelj and Tim Mitchison for their comments and suggestions, Bob Morris for assistance in image quantification, and Rudolf Oldenbourg and Grant Harris for their assistance with LC-Polscope imaging at the Marine Biological Laboratory. This work is supported by S06 GM08136, GM61222, P20 RR16480, and the Robert Day Allen- and Baxter Fellowships at the Marine Biological Laboratory.

Supporting Information Available: This material is available free of charge *via* the Internet at http://pubs.acs.org.

REFERENCES

1. Watson, C. S., Bulayeva, N. N., Wozniak, A. L., and Alyea, R. A. (2006) Steroids.
2. Colborn, T., vom Saal, F. S., and Soto, A. M. (1993) Developmental effects of endocrine-disrupting chemicals in wildlife and humans, *Environ. Health Perspect. 101*, 378–384.

3. Hawley, R. S., and Warburton, D. (2007) Scrambling Eggs in Plastic Bottles, *PLoS Genet. 3*, e6.
4. vom Saal, F. S., and Hughes, C. (2005) Endocrine disruptors and reproductive health: the case of bisphenol-A, *Environ. Health Perspect. 113*, 926–933.
5. Maffini, M. V., Rubin, B. S., Sonnenschein, C., and Soto, A. M. (2006) An extensive new literature concerning low-dose effects of bisphenol A shows the need for a new risk assessment, *Mol. Cell. Endocrinol. 254–255*, 179–186.
6. Roy, D., Palangat, M., Chen, C. W., Thomas, R. D., Colerangle, J., Atkinson, A., and Yan, Z. J. (1997) Biochemical and molecular changes at the cellular level in response to exposure to environmental estrogen-like chemicals, *J. Toxicol. Environ. Health 50*, 1–29.
7. Brotons, J. A., Olea-Serrano, M. F., Villalobos, M., Pedraza, V., and Olea, N. (1995) Xenoestrogens released from lacquer coatings in food cans, *Environ. Health Perspect. 103*, 608–612.
8. Fung, E. Y., Ewoldsen, N. O., St Germain, H. A., Jr., Marx, D. B., Miaw, C. L., Siew, C., Chou, H. N., Gruninger, S. E., and Meyer, D. M. (2000) Pharmacokinetics of bisphenol A released from a dental sealant, *J. Am. Dent Assoc., JADA 131*, 51–58.
9. Krishnan, A. V., Stathis, P., Permuth, S. F., Tokes, L., and Feldman, D. (1993) Bisphenol-A: An estrogenic substance is released from polycarbonate flasks during autoclaving, *Endocrinology 132*, 2279–2286.
10. Susiarjo, M., Hassold, T. J., Freeman, E., and Hunt, P. A. (2007) Bisphenol A exposure causes meiotic aneuploidy in the female mouse, *PLoS Genet. 3*, e5.
11. Hunt, P. A., Koehler, K. E., Susiarjo, M., Hodges, C. A., Ilagan, A., Voigt, R. C., Thomas, S., Thomas, B. F., and Hassold, T. J. (2003) Bisphenol A exposure in utero disrupts early oogenesis in the mouse, *Curr. Biol. 13*, 546–553.
12. Ho, S. M., Tang, W. Y., Belmonte de Frausto, J., and Prins, G. S. (2006) Developmental exposure to estradiol and bisphenol A increases susceptibility to prostate carcinogenesis and epigenetically regulates phosphodiesterase type 4 variant 4, *Cancer Res. 66*, 5624–5632.
13. Prins, G. S., Birch, L., Tang, W. Y., and Ho, S. M. (2007) Developmental estrogen exposures predispose to prostate carcinogenesis with aging, *Reprod. Toxicol. 23*, 374–382.
14. Tsutsui, T., and Barrett, J. C. (1997) Neoplastic transformation of cultured mammalian cells by estrogens and estrogenlike chemicals, *Environ. Health Perspect. 105*, Suppl 3619–624.
15. Tsutsui, T., Tamura, Y., Suzuki, A., Hirose, Y., Kobayashi, M., Nishimura, H., Metzler, M., and Barrett, J. C. (2000) Mammalian cell transformation and aneuploidy induced by five bisphenols, *Int. J. Cancer 86*, 151–154.
16. Tsutsui, T., Tamura, Y., Yagi, E., Hasegawa, K., Takahashi, M., Maizumi, N., Yamaguchi, F., and Barrett, J. C. (1998) Bisphenol-A induces cellular transformation, aneuploidy and DNA adduct formation in cultured Syrian hamster embryo cells, *Int. J. Cancer 75*, 290–294.
17. Andersen, M., Kiel, P., Larsen, H., and Maxild, J. (1978) Mutagenic action of aromatic epoxy resins, *Nature 276*, 391–392.
18. Ochi, T. (1999) Bisphenol A and its methylated congeners inhibit growth and interfere with microtubules in human fibroblasts in vitro, *Mutat. Res. 431*, 105–121.
19. Lehmann, L., and Metzler, M. (2004) Effects of estrogens on microtubule polymerization in vitro: correlation with estrogenicity, *Chem. Biol. Interact. 147*, 273–285.
20. Metzler, M., and Pfeiffer, E. (1995) Induction of multiple microtubule-organizing centers, multipolar spindles and multipolar division in cultured V79 cells exposed to diethylstilbestrol, estradiol-17beta and bisphenol A, *Environ. Health Perspect. 103*, Suppl 721–22.
21. Parry, E. M., Parry, J. M., Corso, C., Doherty, A., Haddad, F., Hermine, T. F., Johnson, G., Kayani, M., Quick, E., Warr, T., and Williamson, J. (2002) Detection and characterization of mechanisms of action of aneugenic chemicals, *Mutagenesis 17*, 509–521.
22. Nakagomi, M., Suzuki, E., Usumi, K., Saitoh, Y., Yoshimura, S., Nagao, T., and Ono, H. (2001) Bisphenol-A induces cell cycle delay and alters centrosome and spindle microtubular organization in oocytes during meiosis, *Teratog., Carcinog., Mutagen. 21*, 453–462.
23. Can, A., Semiz, O., and Cinar, O. (2005) Effects of endocrine disrupting chemicals on the microtubule network in Chinese hamster V79 cells in culture and in Sertoli cells in rats, *Mol. Hum. Reprod. 11*, 389–396.
24. Pfeiffer, E., Rosenberg, B., Deuschel, S., and Metzler, M. (1997) Interference with microtubules and induction of micronuclei in vitro by various bisphenols, *Mutat. Res. 390*, 21–31.
25. Steiner, S., Honger, G., and Sagelsdorff, P. (1992) In vitro conversion of environmental estrogenic chemical bisphenol A to DNA binding metabolite(s), *Carcinogenesis 13*, 969–972.
26. Iso, T., Watanabe, T., Iwamoto, T., Shimamoto, A., and Furuichi, Y. (2006) The reaction of bisphenol A 3,4-quinone with DNA, *Biol. Pharm. Bull. 29*, 206–210.
27. Edmonds, J. S., Nomachi, M., Terasaki, M., Morita, M., Skelton, B. W., and White, A. H. (2004) DNA damage caused by bisphenol A and estradiol through estrogenic activity, *Biochem. Biophys. Res. Commun. 319*, 556–561.
28. Atkinson, A., and Roy, D. (1995) Molecular dosimetry of DNA adducts in C3H mice treated with bisphenol A diglycidylether, *Biochem. Biophys. Res. Commun. 210*, 424–433.
29. Roepke, T. A., Snyder, M. J., and Cherr, G. N. (2005) Estradiol and endocrine disrupting compounds adversely affect development of sea urchin embryos at environmentally relevant concentrations, *Aquat. Toxicol. 71*, 155–173.
30. Gross, P. R. (1964) The immediacy of genomic control during early development, *J. Exp. Zool. 157*, 21–38.
31. Rappaport, R. (1996) *Cytokinesis in Animal Cells*, Cambridge University Press, Cambridge.
32. Burgess, D. R., and Chang, F. (2005) Site selection for the cleavage furrow at cytokinesis, *Trends Cell Biol. 15*, 156–162.
33. Oldenbourg, R. (1999) Polarized light microscopy of spindles, *Methods Cell Biol. 61*, 175–208.
34. Inoue, S., and Oldenbourg, R. (1998) Microtubule dynamics in mitotic spindle displayed by polarized light microscopy, *Mol. Biol. Cell 9*, 1603–7.
35. Gao, H., Katzenellenbogen, J. A., Garg, R., and Hansch, C. (1999) Comparative QSAR analysis of estrogen receptor ligands, *Chem. Rev. 99*, 723–744.
36. Fang, H., Tong, W., Shi, L. M., Blair, R., Perkins, R., Branham, W., Hass, B. S., Xie, Q., Dial, S. L., Moland, C. L., and Sheehan, D. M. (2001) Structure-activity relationships for a large diverse set of natural, synthetic, and environmental estrogens, *Chem. Res. Toxicol. 14*, 280–294.
37. Anstead, G. M., Carlson, K. E., and Katzenellenbogen, J. A. (1997) The estradiol pharmacophore: ligand structure-estrogen receptor binding affinity relationships and a model for the receptor binding site, *Steroids 62*, 268–303.
38. Corona, C., Bryant, B. K., and Arterburn, J. B. (2006) Synthesis of a biotin-derived alkyne for pd-catalyzed coupling reactions, *Org. Lett. 8*, 1883–1886.
39. Longo, F. J., Mathews, L., and Palazzo, R. E. (1994) Sperm nuclear transformations in cytoplasmic extracts from surf clam (*Spisula solidissima*) oocytes, *Dev. Biol. 162*, 245–258.
40. Palazzo, R. E., Vaisberg, E., Cole, R. W., and Rieder, C. L. (1992) Centriole duplication in lysates of *Spisula solidissima* oocytes, *Science 256*, 219–221.

41. Desai, A., Murray, A., Mitchison, T. J., and Walczak, C. E. (1999) The use of Xenopus egg extracts to study mitotic spindle assembly and function in vitro, *Methods Cell Biol. 61*, 385–412.
42. Herzog, W., and Weber, K. (1977) In vitro assembly of pure tubulin into microtubules in the absence of microtubule-associated proteins and glycerol, *Proc. Natl. Acad. Sci. U.S.A. 74*, 1860–1864.
43. Shelanski, M. L., Gaskin, F., and Cantor, C. R. (1973) Microtubule assembly in the absence of added nucleotides, *Proc. Natl. Acad. Sci. U.S.A. 70*, 765–768.
44. Zimmerman, W. C., Sillibourne, J., Rosa, J., and Doxsey, S. J. (2004) Mitosis-specific anchoring of gamma tubulin complexes by pericentrin controls spindle organization and mitotic entry, *Mol. Biol. Cell 15*, 3642–3657.
45. Coleman, K. P., Toscano, W. A., and Wiese, T. E. (2003) QSAR models of the in vitro estrogen activity of Bisphenol A analogs, *QSAR Comb. Sci. 22*, 78–88.
46. Doxsey, S. (2002) Duplicating dangerously: linking centrosome duplication and aneuploidy, *Mol. Cell 10*, 439–440.
47. Kramer, A., Neben, K., and Ho, A. D. (2002) Centrosome replication, genomic instability and cancer, *Leukemia 16*, 767–775.
48. Khodjakov, A., Cole, R. W., Oakley, B. R., and Rieder, C. L. (2000) Centrosome-independent mitotic spindle formation in vertebrates, *Curr. Biol. 10*, 59–67.
49. Merdes, A., Ramyar, K., Vechio, J. D., and Cleveland, D. W. (1996) A complex of NuMA and cytoplasmic dynein is essential for mitotic spindle assembly, *Cell 87*, 447–458.
50. Ivett, J. L., Brown, B. M., Rodgers, C., Anderson, B. E., Resnick, M. A., and Zeiger, E. (1989) Chromosomal aberrations and sister chromatid exchange tests in Chinese hamster ovary cells in vitro. IV. Results with 15 chemicals, *Environ. Mol. Mutagen. 14*, 165–187.
51. Giet, R., Petretti, C., and Prigent, C. (2005) Aurora kinases, aneuploidy and cancer, a coincidence or a real link? *Trends Cell Biol. 15*, 241–50.
52. Weaver, B. A., and Cleveland, D. W. (2006) Does aneuploidy cause cancer? *Curr. Opin. Cell Biol. 18*, 658–667.
53. Echard, A., Hickson, G. R., Foley, E., and O'Farrell, P. H. (2004) Terminal cytokinesis events uncovered after an RNAi screen, *Curr. Biol. 14*, 1685–93.
54. Goshima, G., and Vale, R. D. (2003) The roles of microtubule-based motor proteins in mitosis: comprehensive RNAi analysis in the Drosophila S2 cell line, *J. Cell Biol. 162*, 1003–1016.
55. Goshima, G., Wollman, R., Goodwin, S. S., Zhang, N., Scholey, J. M., Vale, R. D., and Stuurman, N. (2007) Genes required for mitotic spindle assembly in Drosophila S2 cells, *Science 316*, 417–421.
56. Skop, A. R., Liu, H., Yates, J., 3rd, Meyer, B. J., and Heald, R. (2004) Dissection of the mammalian midbody proteome reveals conserved cytokinesis mechanisms, *Science 305*, 61–66.
57. Bodmer, D. M., Tiefenauer, L. X., and Andres, R. Y. (1989) Antigen-versus antibody-immobilized ELISA procedures based on a biotinyl-estradiol conjugate, *J. Steroid Biochem. 33*, 1161–1166.
58. Hauptmann, H., Metzger, J., Schnitzbauer, A., Cuilleron, C. Y., Mappus, E., and Luppa, P. B. (2003) Syntheses and ligand-binding studies of 1 alpha- and 17 alpha-aminoalkyl dihydrotestosterone derivatives to human sex hormone-binding globulin, *Steroids 68*, 629–639.
59. Hauptmann, H., Paulus, B., Kaiser, T., Herdtweck, E., Huber, E., and Luppa, P. B. (2000) Concepts for the syntheses of biotinylated steroids. Part I: testosterone derivatives as immunochemical probes, *Bioconjugate Chem. 11*, 239–252.
60. Hauptmann, H., Paulus, B., Kaiser, T., and Luppa, P. B. (2000) Concepts for the syntheses of biotinylated steroids. Part II: 17beta-estradiol derivatives as immunochemical probes, *Bioconjugate Chem. 11*, 537–548.
61. Hussey, S. L., Muddana, S. S., and Peterson, B. R. (2003) Synthesis of a beta-estradiol-biotin chimera that potently heterodimerizes estrogen receptor and streptavidin proteins in a yeast three-hybrid system, *J. Am. Chem. Soc. 125*, 3692–3693.
62. Kaiser, T., Gudat, P., Stock, W., Pappert, G., Grol, M., Neumeier, D., and Luppa, P. B. (2000) Biotinylated steroid derivatives as ligands for biospecific interaction analysis with monoclonal antibodies using immunosensor devices, *Anal. Biochem. 282*, 173–185.
63. Lacorn, M., Fleischer, K., Willig, S., Gremmel, S., Steinhart, H., and Claus, R. (2005) Use of biotinylated 17beta-estradiol in enzyme-immunoassay development: spacer length and chemical structure of the bridge are the main determinants in simultaneous streptavidin-antibody binding, *J. Immunol. Methods 297*, 225–236.
64. Luppa, P., Birkmayer, C., and Hauptmann, H. (1994) Synthesis of 3-hydroxyestra-1,3,5(10)-trien-17-one and 3,17 beta-dihydroxyestra-1,3,5(10)-triene 6 alpha-N-(epsilon-biotinyl) caproamide, tracer substances for developing immunoassays for estrone and estradiol, *Bioconjugate Chem. 5*, 167–171.
65. Luppa, P., Hauck, S., Schwab, I., Birkmayer, C., and Hauptmann, H. (1996) Synthesis of 17 beta-hydroxyandrost-4-en-3-one-7 alpha-(biotinyl-6-N-hexylamide), a conjugate useful for affinity chromatography and for testosterone immunoassays, *Bioconjugate Chem. 7*, 332–7.
66. Mares, A., DeBoever, J., Stans, G., Bosmans, E., and Kohen, F. (1995) Synthesis of a novel biotin-estradiol conjugate and its use for the development of a direct, broad range enzyme immunoassay for plasma estradiol, *J. Immunol. Methods 183*, 211–219.
67. Muddana, S. S., and Peterson, B. R. (2004) Facile synthesis of cids: biotinylated estrone oximes efficiently heterodimerize estrogen receptor and streptavidin proteins in yeast three hybrid systems, *Org. Lett. 6*, 1409–1412.
68. Tiefenauer, L. X., and Andres, R. Y. (1990) Biotinyl-estradiol derivatives in enzyme immunoassays: structural requirements for optimal antibody binding, *J. Steroid Biochem. 35*, 633–639.
69. Wang, S., Lin, S., Du, L., and Zhuang, H. (2006) Flow injection chemiluminescence immunoassay for 17beta-estradiol using an immunoaffinity column, *Anal. Bioanal. Chem. 384*, 1186–1190.
70. Zhao, J., Wang, Y., Mi, J., Li, Y., and Chang, W. (2003) Sensitive ELISA for determination of serum E2 using a new tracer E2-Biotin, *J. Immunoassay Immunochem. 24*, 369–382.
71. Sato, S., Kwon, Y., Kamisuki, S., Srivastava, N., Mao, Q., Kawazoe, Y., and Uesugi, M. (2007) Polyproline-rod approach to isolating protein targets of bioactive small molecules: isolation of a new target of indomethacin, *J. Am. Chem. Soc. 129*, 873–880.
72. Redeuilh, G., Secco, C., and Baulieu, E. E. (1985) The use of the biotinyl estradiol-avidin system for the purification of "nontransformed" estrogen receptor by biohormonal affinity chromatography, *J. Biol. Chem. 260*, 3996–4002.
73. Eisen, C., Meyer, C., Dressendorfer, R., Strasburger, C., Decker, H., and Wehling, M. (1996) Biotin-labelled and photoactivatable aldosterone and progesterone derivatives as ligands for affinity chromatography, fluorescence immunoassays and photoaffinity labelling, *Eur. J. Biochem. 237*, 514–8.
74. Schirrmacher, E., Beck, C., Brueckner, B., Schmitges, F., Siedlecki, P., Bartenstein, P., Lyko, F., and Schirrmacher, R. (2006) Synthesis and in vitro evaluation of biotinylated RG108: a high affinity compound for studying binding interactions with human DNA methyltransferases, *Bioconjugate Chem. 17*, 261–266.
75. Honda, T., Janosik, T., Honda, Y., Han, J., Liby, K. T., Williams, C. R., Couch, R. D., Anderson, A. C., Sporn, M. B., and Gribble, G. W. (2004) Design, synthesis, and biological evaluation of biotin conjugates of 2-cyano-3,12-dioxooleana-1,9(11)-dien-28-oic acid for the isolation of the protein targets, *J. Med. Chem. 47*, 4923–4932.

76. Dargis, M., and Malouin, F. (1994) Use of biotinylated beta-lactams and chemiluminescence for study and purification of penicillin-binding proteins in bacteria, *Antimicrob. Agents Chemother. 38*, 973–980.
77. Sharp, D. C., and Parry, J. M. (1985) Diethylstilboestrol: the binding and effects of diethylstilboestrol upon the polymerisation and depolymerisation of purified microtubule protein in vitro, *Carcinogenesis 6*, 865–871.
78. Hartley-Asp, B., Deinum, J., and Wallin, M. (1985) Diethylstilbestrol induces metaphase arrest and inhibits microtubule assembly, *Mutat. Res. 143*, 231–235.
79. Wheeler, W. J., Cherry, L. M., Downs, T., and Hsu, T. C. (1986) Mitotic inhibition and aneuploidy induction by naturally occurring and synthetic estrogens in Chinese hamster cells in vitro, *Mutat. Res. 171*, 31–41.
80. Tucker, R. W., and Barrett, J. C. (1986) Deceased numbers of spindle and cytoplasmic microtubules in hamster embryo cells treated with a carcinogen, diethylstilbestrol, *Cancer Res. 46*, 2088–2095.
81. Desai, A., and Mitchison, T. J. (1997) Microtubule polymerization dynamics, *Annu. Rev. Cell Dev. Biol. 13*, 83–117.
82. Beker-van Woudenberg, A. R., van Tol, H. T., Roelen, B. A., Colenbrander, B., and Bevers, M. M. (2004) Estradiol and its membrane-impermeable conjugate (estradiol-bovine serum albumin) during in vitro maturation of bovine oocytes: effects on nuclear and cytoplasmic maturation, cytoskeleton, and embryo quality, *Biol. Reprod. 70*, 1465–1474.
83. Miyoshi, Y., Iwao, K., Egawa, C., and Noguchi, S. (2001) Association of centrosomal kinase STK15/BTAK mRNA expression with chromosomal instability in human breast cancers, *Int. J. Cancer 92*, 370–373.
84. Lo, Y. L., Yu, J. C., Chen, S. T., Yang, H. C., Fann, C. S., Mau, Y. C., and Shen, C. Y. (2005) Breast cancer risk associated with genotypic polymorphism of the mitosis-regulating gene Aurora-A/STK15/BTAK, *Int. J. Cancer 115*, 276–283.
85. Li, J. J., Weroha, S. J., Lingle, W. L., Papa, D., Salisbury, J. L., and Li, S. A. (2004) Estrogen mediates Aurora-A overexpression, centrosome amplification, chromosomal instability, and breast cancer in female ACI rats, *Proc. Natl. Acad. Sci. U.S.A. 101*, 18123–18128.
86. Hontz, A. E., Li, S. A., Lingle, W. L., Negron, V., Bruzek, A., Salisbury, J. L., and Li, J. J. (2007) Aurora a and B overexpression and centrosome amplification in early estrogen-induced tumor foci in the Syrian hamster kidney: implications for chromosomal instability, aneuploidy, and neoplasia, *Cancer Res. 67*, 2957–2963.
87. Goepfert, T. M., Adigun, Y. E., Zhong, L., Gay, J., Medina, D., and Brinkley, W. R. (2002) Centrosome amplification and overexpression of aurora A are early events in rat mammary carcinogenesis, *Cancer Res. 62*, 4115–4122.
88. Dai, Q., Cai, Q. Y., Shu, X. O., Ewart-Toland, A., Wen, W. Q., Balmain, A., Gao, Y. T., and Zheng, W. (2004) Synergistic effects of STK15 gene polymorphisms and endogenous estrogen exposure in the risk of breast cancer, *Cancer Epidemiol. Biomarkers Prev. 13*, 2065–2070.
89. Li, D., Zhu, J., Firozi, P. F., Abbruzzese, J. L., Evans, D. B., Cleary, K., Friess, H., and Sen, S. (2003) Overexpression of oncogenic STK15/BTAK/Aurora A kinase in human pancreatic cancer, *Clin. Cancer Res. 9*, 991–997.
90. Meraldi, P., Honda, R., and Nigg, E. A. (2004) Aurora kinases link chromosome segregation and cell division to cancer susceptibility, *Curr. Opin. Genet. Dev. 14*, 29–36.
91. Shuster, C. B., and Burgess, D. R. (2002) Transitions regulating the timing of cytokinesis in embryonic cells, *Curr. Biol. 12*, 854–858.
92. Hinchcliffe, E. H., Cassels, G. O., Rieder, C. L., and Sluder, G. (1998) The coordination of centrosome reproduction with nuclear events of the cell cycle in the sea urchin zygote, *J. Cell Biol. 140*, 1417–1426.
93. Sluder, G., and Rieder, C. L. (1985) Centriole number and the reproductive capacity of spindle poles, *J. Cell Biol. 100*, 887–896.
94. Megraw, T. L., Kao, L. R., and Kaufman, T. C. (2001) Zygotic development without functional mitotic centrosomes, *Curr. Biol. 11*, 116–120.
95. Heald, R., Tournebize, R., Blank, T., Sandaltzopoulos, R., Becker, P., Hyman, A., and Karsenti, E. (1996) Self-organization of microtubules into bipolar spindles around artificial chromosomes in Xenopus egg extracts, *Nature 382*, 420–425.
96. Heald, R., Tournebize, R., Habermann, A., Karsenti, E., and Hyman, A. (1997) Spindle assembly in Xenopus egg extracts: respective roles of centrosomes and microtubule self-organization, *J. Cell Biol. 138*, 615–628.
97. Merdes, A., Heald, R., Samejima, K., Earnshaw, W. C., and Cleveland, D. W. (2000) Formation of spindle poles by dynein/dynactin-dependent transport of NuMA, *J. Cell Biol. 149*, 851–862.
98. Manning, A. L., and Compton, D. A. (2007) Mechanisms of spindle-pole organization are influenced by kinetochore activity in mammalian cells, *Curr. Biol. 17*, 260–265.
99. Stack, C., Lucero, A. J., and Shuster, C. B. (2006) Calcium-responsive contractility during fertilization in sea urchin eggs, *Dev. Dyn. 235*, 1042–1052.
100. Lucero, A., Stack, C., Bresnick, A. R., and Shuster, C. B. (2006) A global, myosin light chain kinase-dependent increase in myosin II contractility accompanies the metaphase-anaphase transition in sea urchin eggs, *Mol. Biol. Cell 17*, 4093–4104.
101. Wong, G. K., Allen, P. G., and Begg, D. A. (1997) Dynamics of filamentous actin organization in the sea urchin egg cortex during early cleavage divisions: implications for the mechanism of cytokinesis, *Cell Motil. Cytoskeleton 36*, 30–42.
102. Murray, A. W. (1991) Cell cycle extracts, *Methods Cell Biol. 36*, 581–605.
103. Gliksman, N. R., Parsons, S. F., and Salmon, E. D. (1993) Cytoplasmic extracts from the eggs of sea urchins and clams for the study of microtubule-associated motility and bundling, *Methods Cell Biol. 39*, 237–251.
104. George, O., Johnston, M. A., and Shuster, C. B. (2006) Aurora B kinase maintains chromatin organization during the MI to MII transition in surf clam oocytes, *Cell Cycle 5*, 2648–2656.
105. Palazzo, R. E., and Vogel, J. M. (1999) Isolation of centrosomes from Spisula solidissima oocytes, *Methods Cell Biol. 61*, 35–56.